

Calculated Optical Properties of RuO₂

T. D. Williams, D. Bagayoko, and G. L. Zhao

ABSTRACT.

We performed a first-principle, computational study of the optical properties of ruthenium dioxide. Our method employed a local density potential and the linear combination of atomic orbitals (LCAO). We circumvented a recently discovered spurious effect that is inherently associated with basis sets in variational calculations of the Rayleigh-Ritz type. Consequently, a significantly new feature of our method consists of the implementation of the Bagayoko, Zhao, and Williams (BZW) procedure. We present our findings on the electronic structure and the optical properties of RuO₂. We provide detailed computational results on the real and imaginary part of the dielectric function. We compare these results with experimental measurements. To our knowledge, this work reports the first theoretical results on the dielectric function of RuO₂. The agreement with measurements, within the applicable uncertainties, is very good.

I. INTRODUCTION

Ruthenium dioxide (RuO_2) is a member of the transition metal oxide family. RuO_2 has a rutile structure and exhibits metallic conductivity. The metallic nature of ruthenium dioxide led to its wide range of use in industry. The conductive behavior of ruthenium dioxide suggests that it may be used as an electrical contact material.[1] It is used in the chlor-alkali industry as an electrocatalyst.[2] RuO_2 is also used in integrated circuits as an electrode conductor.[3] It is the most environmentally stable member of the transition metal oxide family. The properties of RuO_2 suggest that it may be used as an optical thin film. Ruthenium dioxide is also used in ceramic resistors.[4] It is widely utilized in the photodecomposition of water.[5] Thin films of ruthenium dioxide have shown exceptional diffusion barrier properties.[6]

Tetragonal RuO_2 is a member of the $P_{4_2}/\text{mmn}(D_{2h}^{14})$ space group. [7] RuO_2 has six atoms per unit cell, two ruthenium and four oxygen. The lattice constants of ruthenium dioxide in atomic units are $a = 8.4884600$, $c = 5.87062750$, and $u = 0.306$. [8] The ruthenium atoms are located at the Wyckoff 2(a) sites, $(0,0,0)$ and $(\frac{1}{2}, \frac{1}{2}, \frac{1}{2})$. The oxygen atoms occupy the Wyckoff 4(f) sites, $\pm(u + \frac{1}{2}, \frac{1}{2} - u, \frac{1}{2})$ and $\pm(u, u, 0)$. We discuss below some currently

available studies of this important material.

Goel et al.[3] measured various optical properties of a single crystal of RuO_2 at room temperature, including the real and imaginary part of the dielectric function. Belkind et al. performed similar measurements on RuO_2 thin films.[10]. More recently, Mondio et al. performed reflective electron energy loss spectroscopy (REELS) on RuO_2 thin films.[11] Their results, for the dielectric function, strongly agreed with those of Goel et al. The above authors discussed other experimental investigations of ruthenium dioxide.[19, 20, 21].

Several theoretical studies[2, 8, 18, 25] of the electronic and related properties of ruthenium dioxide followed the pioneering work of Mattheiss.[9] Glassford and Chelikowsky[2] reviewed these calculations to show a general agreement similar to that between the experimental works, on the one hand, and a significant agreement between theoretical and measured results, on the other hand. The emerging consensus on the properties of RuO_2 suffers, however, from the absence of theoretical results on key measures of the optical properties of the materials, namely, the real and imaginary parts of the dielectric function.

A central aim of this work is to provide ab-initio, theoretical results for

the dielectric function of RuO₂. It is expected that comparison with the single crystal[3] and thin film[10, 11] measurements will add to our understanding of ruthenium dioxide. An accompanying aim of this work consists of determining the corrections, if any, the application of a newly introduced computational procedure[15, 16] makes to the calculated band structure and related results for RuO₂.

In the following section, we discuss our computational method. In the third section, we present the calculated results as compared with experimental measurements. The final section is a short conclusion.

II. THE METHOD

2.1 General Method: LDA and LCGO

Our non-relativistic computations employed an expanded version of the electronic structure calculation program package developed at the Department of Energy's (DOE) Ames Laboratory in Iowa.[12, 13] This package utilizes a first-principle LCAO method to perform self-consistent calculations of the electronic structure and optical properties of RuO₂. We selected the

Ceperley and Adler form of the local density approximation as parameterized by Vosko, Wilk, and Nusair[14]. The only effect of temperature possible included in our work is that which stems from using a lattice constant that is not for zero temperature. The first step in the LCAO method, for a solid, is the computation of the atomic wave functions of the various atomic or ionic species represented in the material. In the LCAO method, the electronic eigenstate, $\Psi_{\vec{k}n}(\vec{r})$, is expanded as

$$\Psi_{\vec{k}n}(\vec{r}) = \sum_{\alpha m} C_{\alpha m}(\vec{k}n)\phi_{\alpha m}(\vec{k}, \vec{r}). \quad (1)$$

In this expression, \vec{k} is a wave vector in the Brillouin zone, n is a band index, and $C_{\alpha m}$ is the expansion coefficient of the electron eigenfunction. The Bloch wave function, $\phi_{\alpha m}(\vec{k}, \vec{r})$, for a crystalline solid is expanded using the atomic wave functions as

$$\phi_{\alpha m}(\vec{k}, \vec{r}) = \frac{1}{\sqrt{N}} \sum_l e^{i\vec{k}\cdot\vec{R}_l} u_{\alpha m}(\vec{r} - \vec{\tau}_m - \vec{R}_l), \quad (2)$$

where $u_{\alpha m}$ is an atomic wave function of the α -th state of the m -th atom at the position $\vec{\tau}_m$, and \vec{R}_l is a translation vector.

2.2 The BZW Procedure

The optimal basis set for RuO₂ was selected according to the Bagayoko, Zhao, and Williams (BZW) procedure.[15, 16] The BZW procedure avoids a spurious effect that is inherently associated with

- (a) the use of larger and larger basis sets to meet the requirements for completeness,
- (b) the utilization of the wave functions – for the occupied states only – in constructing the charge density in going from one iteration to the next, and
- (c) the mathematical property of the Rayleigh-Ritz variational method consisting of lowering the calculated eigenvalues, toward the corresponding true eigenvalues, as the size of the basis set increases.

As explained by Bagayoko, Zhao, and Williams[15] and Bagayoko et al.[16], the spurious effect consists of the unphysical lowering of some *unoccupied* energy levels, upon an increase of the size of the basis set beyond the optimal size. Of course, any lowering of unoccupied levels – before the convergence of the occupied states – is assumed to be due to actual, physical interactions.

The BZW procedure calls for performing three or more self-consistent calculations with basis sets of different sizes. One generally begins with the

minimal basis set that is limited to the atomic orbitals needed to describe the bare atoms or ions present in the system. Subsequent calculations utilize basis sets that include the minimal basis set plus additional orbitals for unoccupied atomic levels. Table 1 shows the basis sets employed in our calculation. The optimal basis set is defined as the smallest basis set for which the occupied energy levels are "converged" with respect to the size of the basis set. The optimal basis set for RuO_2 is Basis Set II.

There is nothing special about the actual numerical value of the size of this optimal basis set, it varies with the quality of the trial basis functions. Additionally, the use of contractions of orbitals[24] reduces the numerical value of the dimension of the resulting Hamiltonian without changing our conclusions. As explained by Bagayoko, basis set contractions lead to an upward, rigid shift of the calculated energy levels that is different from the above spurious lowering of unoccupied levels only. This shift is another manifestation of the variational theorem[27] noted above. The essential point in the BZW procedure consists of selecting the optimal basis set based on the convergence of the occupied states as described above.

2.3 Computational Details and the Formalism for Optical Prop-

erties

The computational details for this work are very similar to those of Bagayoko et al.[16]. The lattice constants we chose are given above. The basis sets for each of the five self-consistent calculations are indicated in Table 1. A total of 25-37 iterations were necessary for convergence. The convergence of the potentials was up to 10^{-5} . We considered 60 k-points in the irreducible wedge of the Brillouin zone.

Once accurate energy levels and related wave functions are known, one can calculate most properties of materials[28]. We employed the results of our calculations with the optimal basis set to compute the imaginary part of the dielectric function of RuO_2 . This imaginary part of the dielectric function, $\epsilon_2(\omega)$, is obtained using the Kubo-Greenwood formula[17]:

$$\epsilon_2(\omega) = \frac{8\pi^2 e^2}{3m^2 \hbar \omega^2 \Omega} \sum_{\vec{k}} \sum_{nl} |\langle \Psi_{\vec{k}n}(\vec{r}) | \vec{P} | \Psi_{\vec{k}l}(\vec{r}) \rangle|^2 f_{\vec{k}l} [1 - f_{\vec{k}n}] \delta(\epsilon_{\vec{k}n} - \epsilon_{\vec{k}l} - \hbar\omega), \quad (3)$$

where $\hbar\omega$ is the photon energy, Ω is the volume of the unit cell, and \vec{P} is a momentum operator. The real part of the dielectric function, $\epsilon_1(\omega)$, is

calculated using the Kramers-Kronig (K-K) relation,

$$\epsilon_1(\omega) = 1 + \frac{2}{\pi} P \int_0^\infty \frac{\omega' \epsilon_2(\omega')}{\omega'^2 - \omega^2} d\omega'. \quad (4)$$

III. RESULTS

3.1 Electronic Properties: Negligible BZW Corrections for Metals

Our results for the electronic band and related wave functions are characterized by the following two major points:

- (a) our calculations II through V gave exactly the same results for the valence and low lying conduction bands in Figure 1, and
- (b) these results almost perfectly reproduce those of Reference[2].

The significance of these points stems from the fact that they clearly indicate that corrections expected from the application of the BZW procedure are negligible for metals, unlike in the case of semiconductors.[15, 26, 27]. Consequently, our calculated total density of states (DOS) in Figure 2 are the same as those of Glassford and Chelikowsky[2]—in qualitative and quantitative terms. These authors did not provide the partial density of states (PDOS) we show in Figure 3. These PDOS qualitatively agree with some results of Schwarz[18]. Our PDOS are different from those obtained by Schwarz for energies between -5 and -10 eV. The differences are both qualitative and quantitative. For instance, our calculated PDOS for Ru-4d and O-2p clearly

show double-peaks structure not discernible from the augmented spherical wave (ASW) results of Schwarz. The magnitudes of the peaks in Figure 3, between -5 and -10 eV, are more than double the corresponding ones as obtained by Schwarz. We ascribe these discrepancies to differences between our ab-initio calculations and the ASW method.

The negligible nature of the BZW corrections for metals, as illustrated above, pertains only to descriptive calculations. Namely, computations of properties of a material known to be a metal at a given stoichiometric composition and under specified conditions of temperature and pressure. The BZW procedure is expected to be necessary for predictive calculations, i.e., those for materials whose metallic state is not known or for which elemental composition and related concentrations, pressure, or temperature are changed. While no discrepancies were found between our calculations II to V, for the valence and low energy conduction bands, the variational theorem necessarily leads to differences for the highest conduction bands. For instance, the fundamental theorem of algebra dictates that the number of calculated eigen-energies increase as the size of the Hamiltonian increases.

3.2 Optical Properties of RuO₂

The real and imaginary parts of the dielectric function were calculated using the formalism outlined in section 2. We show in Figure 4 and Figure 5 our calculated results, along the direction perpendicular to the z-axis, and the experimental measurements by Goel, Skorinko, and Pollak.[3]

Figure 4 is a plot of the real part of the dielectric function, $\epsilon_1(\omega)$. Our results for $\epsilon_1(\omega)$ are sandwiched between the measurements for a single crystal of RuO₂ and for a thin film of RuO₂. [10] The location of the peaks in $\epsilon_1(\omega)$ show some quantitative and qualitative agreement with experiment. In particular, we reproduce the location of the peaks in the bulk measurement by Goel et al. [3] The absence of intraband transition and of the free electron Drude contributions from our calculated data dictate caution in comparing our results to experiment. The locations of some salient features of the graph are shown in Table 2 .

Figure 5 is a plot of the imaginary part of the dielectric function, $\epsilon_2(\omega)$, versus the photon energy. $\epsilon_2(\omega)$ is calculated using the direct interband transitions between calculated energy levels. The plot also shows experimental measurements by Goel et al. [3] and Belkind et al. [10] The location of the

peaks in $\epsilon_2(\omega)$ show both qualitative and quantitative agreements between our results and the measurements. The correct reproduction of the location of the peaks in the experimental measurements, for $\epsilon_2(\omega)$, is a direct verification of the accuracy of our calculated band structure for occupied and unoccupied energy levels. The differences in magnitude between the experimental measurements and our calculated data may be due, in part, to the effects of temperature, in addition to measured contributions that are not included in the theoretical calculations. The experimental measurements were performed at 300 K and our calculations are for 0 K. Difficulties in the analysis of experimental data are possible sources of differences between the magnitude of experimental data and that of theoretical results. Despite these possible sources of difference, Table 3 shows a good agreement between theory and experiment.

IV. CONCLUSIONS

We performed a first-principle, computational study of the optical properties of RuO₂. We employed a local density potential and the LCAO method. We implemented the BZW procedure to avoid a spurious effect associated with basis sets in variational methods. Our calculated real and imaginary parts of the dielectric function of RuO₂ agree with experiment, within known uncertainties. To our knowledge, our calculations are the first to report theoretical results for the dielectric function of this important oxide. This work indicates that the BZW corrections are expected to be negligible for descriptive, as opposed to predictive, calculations of properties of metals. In particular, this work and related ones[15, 16, 26, 27] strongly point to predictive capabilities of density functional calculations[22, 23], including those based on local density approximation (LDA).

ACKNOWLEDGMENTS

This work was supported in part by funding from the Louisiana Board of Regents Support Fund (BORSF) through a Superior Graduate Fellowship project directed by Dr. D. Bagayoko and Dr. C. H. Yang, Contract No.

LEQSF (1994-98)-GF-18; NASA-USAR; and by the Department of the Navy, Office of Naval Research (ONR, Grant No. N00014-93-1-1368). These fundings were through the Timbuktu Academy, Southern University and A & M College. The Louisiana Board of Regents funded the High Performance Computing Laboratory (HPCL), where part of this work was done [Contract No. LEQSF (1996-97)-ENH-TR-55)].

References

- [1] D. J. Pedder, *Electrocomp. Sci. Tech.* **2**, 259 (1976).
- [2] K. M. Glassford and J. R. Chelikowsky, *Phys. Rev. B.* **47**, 1732 (1993).
- [3] A. K. Goel, G. Skorinko, and F. H. Pollak, *Phys. Rev. B.* **24**, 7342 (1981).
- [4] N. C. Halder, *Electrocomp. Sci. Tech.* **11**, 21 (1983).
- [5] T. Kawai and T. Sakata, *Chem. Phys. Lett.* **72**, 87 (1980).
- [6] L. Krusin-Elbaum, M. Wittmer, and D. S. Yee, *Appl. Phys. Lett.* **50**, 1879 (1987).
- [7] D. B. Rogers, R. D. Shannon, A. W. Sleight, and J. L. Gillson, *Inorg. Chem.* **8**, 841 (1969).
- [8] J. H. Xu, T. Jarlborg, and A. J. Freeman, *Phys. Rev. B* **40**, 7939 (1989).
- [9] L. F. Mattheiss, *Phys. Rev B* **13**, 2433 (1976).
- [10] A. Belkind, Z. Orban, J. L. Vossen, and J. A. Woollam, *Thin Solid Films* **270**, 242 (1992).

- [11] G. Mondio, F. Neri, M. Allegrini, A. Lembo, and F. Fuso, *J. Appl. Phys.* **82**, 1730 (1997).
- [12] G. L. Zhao, T. C. Leung, B. N. Harmon, M. Keil, M. Muller, and W. Weber, *Phys. Rev. B* **40**, 7999 (1989).
- [13] G. L. Zhao and B. N. Harmon, *Phys. Rev. B* **45**, 2818 (1992).
- [14] S. H. Vosko, L. Wilk, and M. Nusair, *Can. J. Phys.* **58**, 1200 (1980).
- [15] D. Bagayoko, G. L. Zhao, and T. D. Williams, *Bulletin of the American Physical Society* **43**, (1998).
- [16] D. Bagayoko, G. L. Zhao, J. D. Fan, J. T. Wang, *J. Phys: Cond. Matt.* **10**, 5645 (1998).
- [17] W. Y. Ching, *J. Am. Ceram. Soc.* **73**, 3135 (1990).
- [18] K. Schwarz, *Phys. Chem. Minerals* **14**, 315 (1987).
- [19] H. L. Park, C. H. Chung, C. H. Kim, and H. S. Kim, *Journal Materials Science Letters* **6**, 1093 (1987).
- [20] J. Riga, C. Tenret-Noel, J. J. Pireaux, R. Cauano, and J. J. Verbist, *Physica Scripta* **16**, 351 (1977).

- [21] R. R. Daniels, G. Margasritondo, C. A. Georg, and F. Levy Phys. Rev. B **29**, 1813 (1984).
- [22] P. Hohenberg and W. Kohn, Phys. Rev. **B136**, 864 (1964).
- [23] W. Kohn and L. J. Sham, Phys. Rev. **A140**, 1133 (1965).
- [24] D. Bagayoko, Inter. J. of Quantum Chemistry **17**, 527 (1983).
- [25] P. I. Sorantin and K. Schwarz, Inorg. Chem. **31**, 567 (1992).
- [26] G. L. Zhao, D. Bagayoko, and T. D. Williams, submitted to Phys. Review B.
- [27] G. L. Zhao, D. Bagayoko, and T. D. Williams, submitted to Phys. Review B.
- [28] J. Callaway, "Quantum Theory of the Solid State", 2nd ed., Academic Press , 1991.

Table 1: The atomic orbitals used in calculations I to V.

Basis Set 0: core-state orbitals in Calculations I to V

Ru(1s, 2s, 3s, 2p, 3p), O(1s)

Basis Set I: Set 0 plus Ru(4s, 5s, 4p, 3d, 4d), O(2s,2p)

Basis Set II: Set I plus Ru(5p⁰), O(3s⁰, 3p⁰)

Basis Set III: Set II plus Ru(6s⁰)

Basis Set IV: Set III plus Ru(6p⁰)

Basis Set V: Set IV plus O(4s⁰)

*Superscript zeros indicate added orbitals representing unoccupied atomic levels.

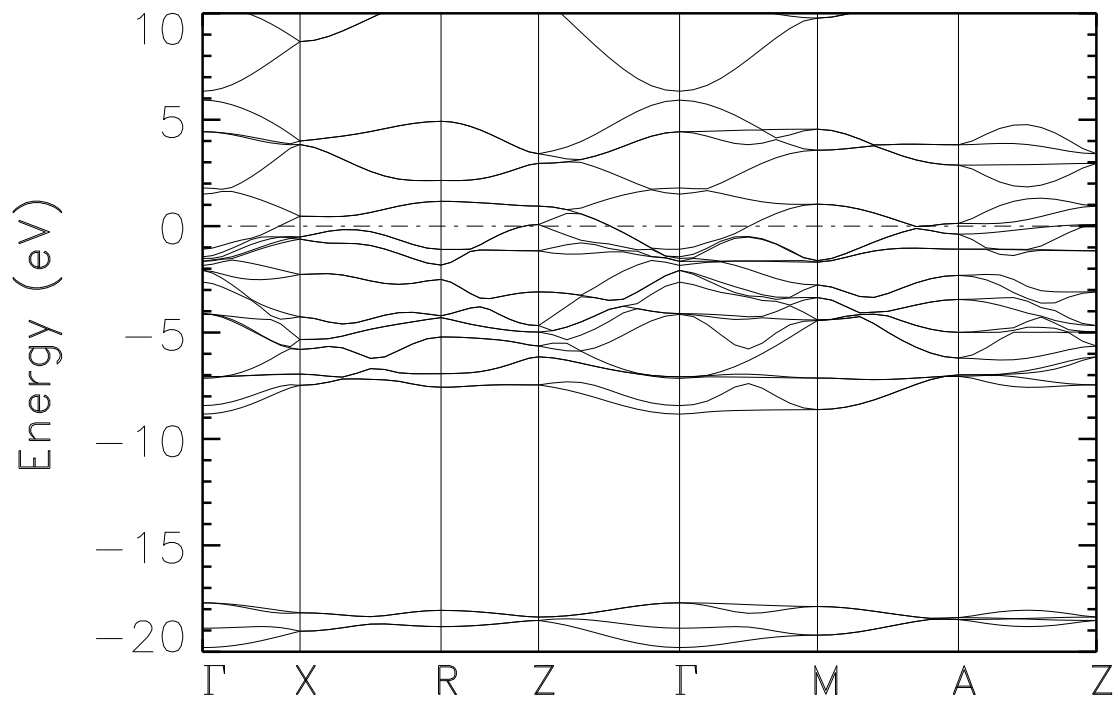


Figure 1: The electronic band structure obtained with the optimal basis set. All results here were obtained with Basis Set II. The shown bands are the same for calculations III-V

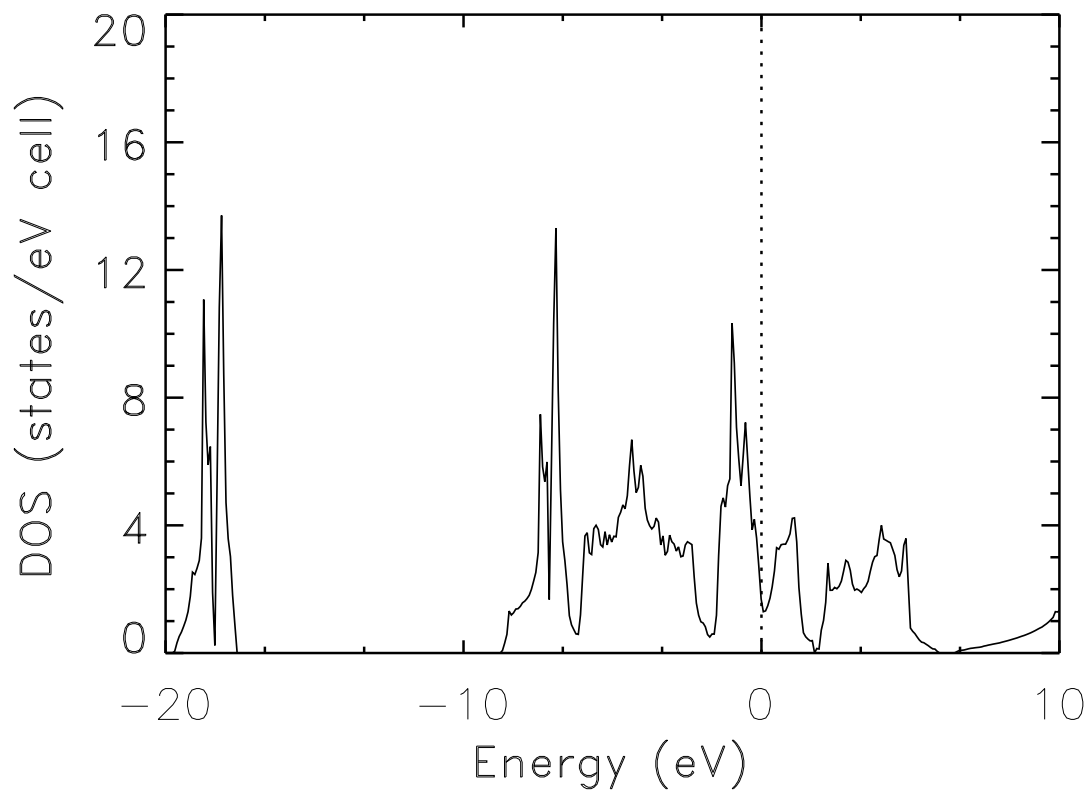


Figure 2: The total density of state (DOS) for RuO₂.

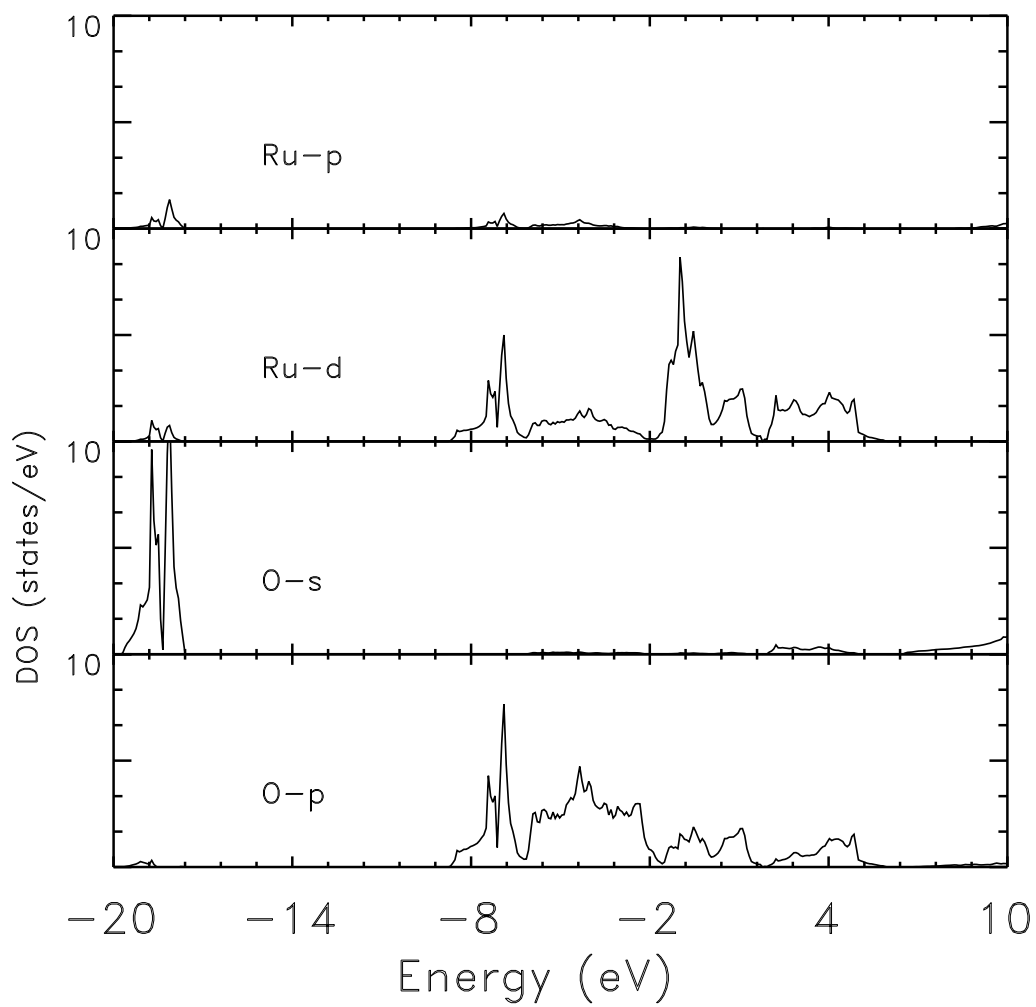


Figure 3: The partial density of state (PDOS) for RuO₂.

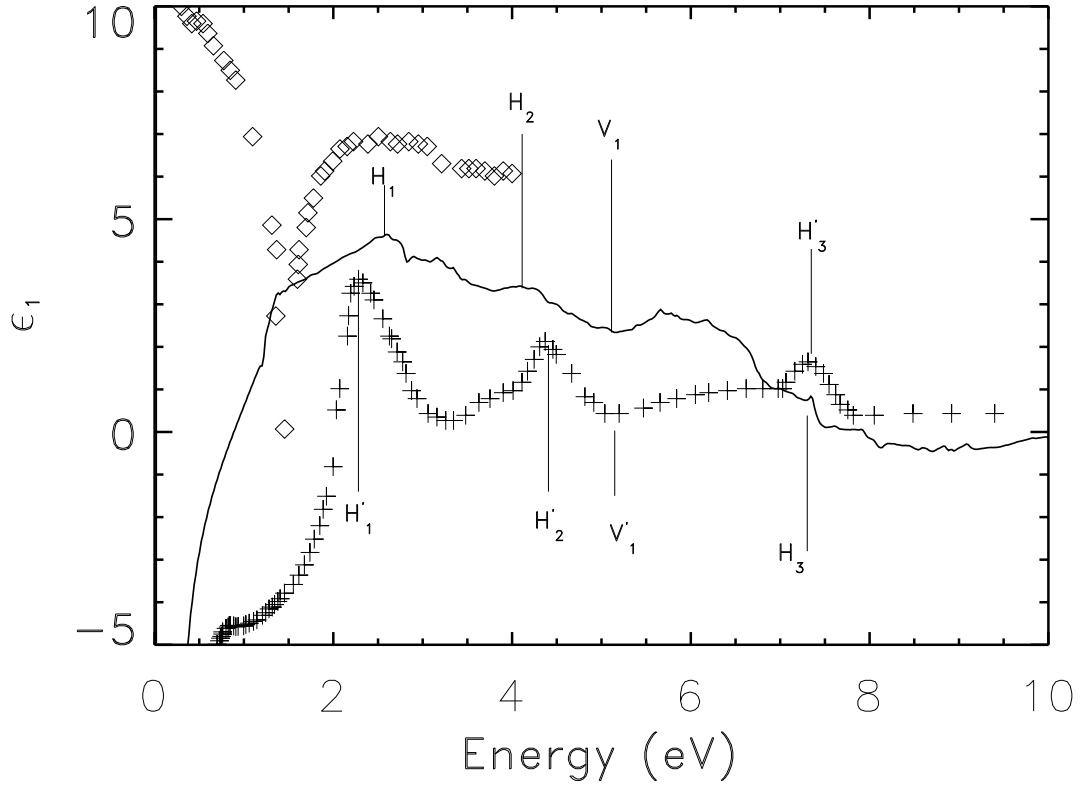


Figure 4: The real part of the dielectric function (ϵ_1). The solid line represents our theoretical results. The experimental data of Goel et al., for rutile, single crystal RuO_2 , with polarization perpendicular to the z-axis, are indicated with (+) while the data from the thin film experiment by Belkind et al. are represented by the diamond symbol (\diamond).

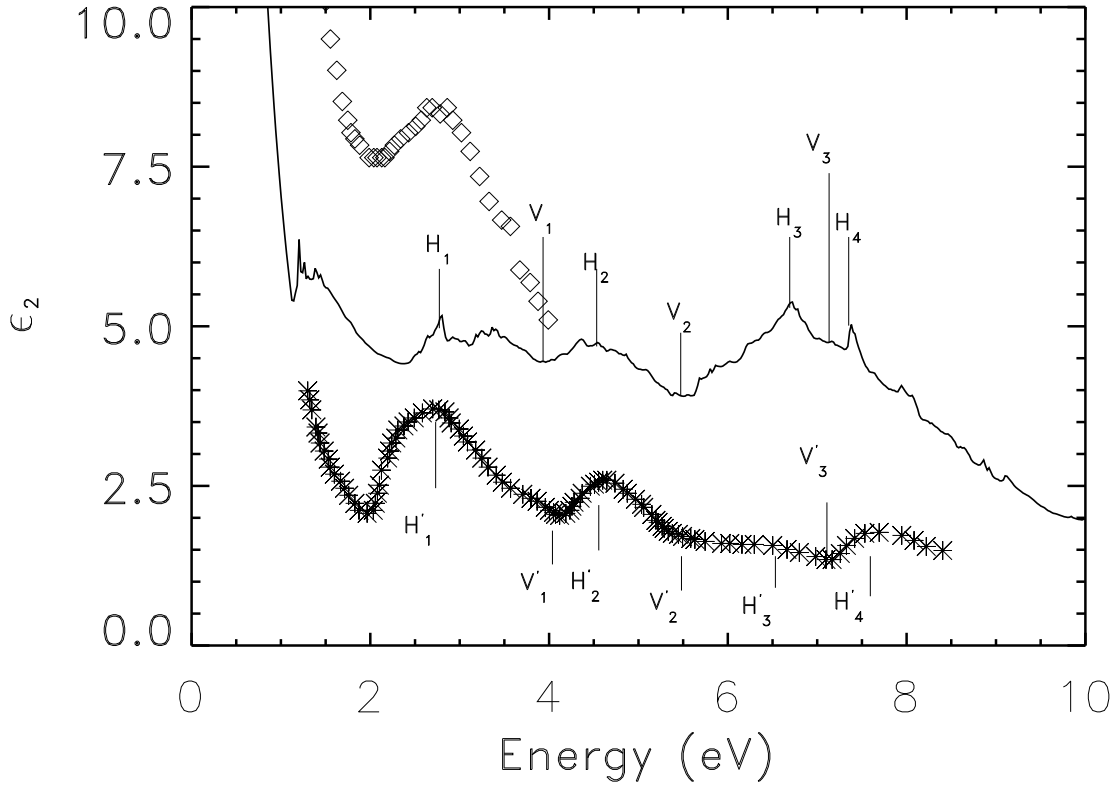


Figure 5: The imaginary part of the dielectric function (ϵ_2). The solid line represents theoretical data. The asterisks (*) represent experimental data from Goel et al.[3] for polarization perpendicular to the z-axis, and the diamond symbols (\diamond) represent the thin film measurement by Belkind et al.[10]

Table 2: Comparison of peak and valley positions in Figure 4 (ϵ_1).

Peak	Calculated	Experiment ^a
H ₁ ,H' ₁	2.603 eV	≈2.28 eV
H ₂ ,H' ₂	4.080 eV	4.37 eV
V ₁ ,V' ₁	5.163 eV	5.19 eV
H ₃ ,V' ₃	7.363 eV	7.31 eV

^a Experimental measurements are by Goel et al. [3] Structures with the superscript (') correspond to experimental data.

Table 3: Comparison of peak and valley positions in Figure 5 (ϵ_2).

Peak	Calculated	Experiment ^a
H ₁ ,H' ₁	2.803 eV	≈2.8 eV
V ₁ ,V' ₁	3.963 eV	4.1 eV
H ₂ ,H' ₂	4.370 eV	4.6 eV
V ₂ ,V' ₂	5.503 eV	5.6 eV
H ₃ ,H' ₃	6.723 eV	6.5 eV
V ₃ ,V' ₃	7.143 eV	7.2 eV
H ₄ ,H' ₄	7.503 eV	7.5 eV

^a Experimental measurements are by Goel et al. [3] Structures with the superscript (') correspond to experimental data.